SERI/TP-253-3426
UC Categories: 202, 235
DE89000837

Heat Transfer and Pressure Drop Measurements in an Air/Molten Salt Direct-Contact Heat Exchanger

Mark S. Bohn

November 1988

Prepared for the ASME
1989 Annual Solar Energy
Division Conference
San Diego, California
2-5 April 1989

Prepared under Task No. ST812331

Solar Energy Research Institute
A Division of Midwest Research Institute

1617 Cole Boulevard
Golden, Colorado 80401-3393

Prepared for the
U.S. Department of Energy
Contract No. DE-AC02-83CH10093

NOTICE

Printed in the United States of America
Available from:
National Technical Information Service
U.S. Department of Commerce
5285 Port Royal Road
Springfield, VA 22161

Price: Microfiche A01
Printed Copy A02

Codes are used for pricing all publications. The code is determined by the number of pages in the publication. Information pertaining to the pricing codes can be found in the current issue of the following publications which are generally available in most libraries: *Energy Research Abstracts (ERA)*; *Government Reports Announcements* and Index *GRA* and I); *Scientific and Technical Abstract Reports (STAR)*; and publication NTIS-PR-360 available from NTIS at the above address.

ABSTRACT

This paper presents a comparison of experimental data with a recently published model of heat exchange in irrigated packed beds. Heat transfer and pressure drop were measured in a 150 mm (ID) column with a 610-mm bed of metal Pall rings. Molten nitrate salt and preheated air were the working fluids with a salt inlet temperature of approximately 440°C and air inlet temper of approximately 230°C. A comparison between the experimental data and the heat transfer model is made on the basis of heat transfer from the salt. For the range of air and salt flow rates tested, 0.3 to 1.2 kg/m^2 s air flow and 6 to 18 kg/m^2 s salt flow, the data agree with the model within 22% standard deviation. In addition, a model for the column pressure drop was validated, agreeing with the experimental data within 18% standard deviation over the range of column pressure drop from 40 to 1250 Pa/m.

NOMENCLATURE

C_s	salt specific heat (Ws/kg K)
C_p	air specific heat (Ws/kg K)
G	gas mass flow per unit cross-sectional area of empty column (kg/m^2 s)
H	column height (m)
Htu	height of a transfer unit (m)
L	salt mass flow per unit cross-sectional area of empty column (kg/m^2 s)
$\dot{m}_s$	salt mass flow rate (kg/s)
Ntu	number of transfer units
Q_{loss}	heat transfer from salt other than that to the air (W)
Q_{outlet}	heat transfer from salt to air below packed bed (W)
Q_s	heat transfer, salt-to-air (W)
Q_{sm}	measured heat transfer, salt-to-air, in packed bed (W)
T_{ai}	air inlet temperature (°C)
T_{ao}	air outlet temperature (°C)
T_{si}	salt inlet temperature (°C)
T_{so}	salt outlet temperature (°C)
Ua	volumetric heat transfer coefficient (W/m^3 K)
V_{hx}	volume of packed bed
ΔT_{LM}	log mean temperature difference

INTRODUCTION

In direct-contact heat exchange heat is transferred from one fluid stream to another by bringing the streams into direct contact with each other. The technology sees widespread use in industry for mass transfer duty in such diverse applications as gas separation, chlorination of hydrocarbons, flue gas scrubbing, etc., but its application to heat transfer duty has been somewhat limited. Potential applications that could benefit from direct-contact heat exchange include waste heat recovery, hot gas quenching, space applications, and solar energy applications. These benefits result from lower first costs, lower operating costs, and applicability to corrosive or fouling fluids and to very high temperature fluids.

Solar energy applications include the central receiver system in which the direct-contact heat exchanger would be used to transfer heat from a liquid-cooled receiver to a gas stream for applications requiring hot gas. A recently proposed central receiver directly heats atmospheric air, and the direct-contact heat exchanger could be used to transfer the heat to high pressure air via a pair of direct-contact heat exchangers. In both cases, the presence of a hot liquid allows one to consider thermal energy storage, which is

generally recognized as necessary for economical operation of a solar thermal plant.

Several methods are available for carrying out the heat exchange, including spray columns, falling film columns, plate columns, and packed beds. The last method is especially effective where low pressure drop or low liquid holdup is important and a high volumetric efficiency is needed. Packed beds are also used for corrosive gas or liquid service or for high temperature applications where plate column internals are not available. A packed bed consists essentially of a vertical column filled with rings, saddles, or other packing material randomly arranged in the column. (Organized column packings, called structured packing, have recently proven beneficial in certain applications.) The liquid is distributed over the top of the bed and trickles down the large surface area of the rings. The gas is pumped counterflow up the bed, and heat transfer takes place primarily at the gas-liquid interface.

Except for very high liquid flow rates, the packed bed remains relatively open, and gas-side pressure drop is very low. Typical operation of these columns involves pressure drop in the range of 400 to 1200 Pa/m, more commonly expressed in terms of 0.5 to 1.5 in. of water column per foot of bed height. As the liquid rate is increased, a larger fraction of the bed flow area is occupied by liquid, and the gas-side pressure drop increases rapidly. Eventually, a point is reached where the liquid is dragged upwards by the gas, resulting in very high pressure drop and poor heat transfer. This point is called flooding.

There are several reasons for the limited application of direct-contact heat exchange. First, the gas and liquid must be compatible in the sense of limited chemical reaction taking place when they are brought into contact with one another. Second, mass transfer between the two streams may be undesirable, further limiting the choice of working fluids. Third, separation of the two streams must be easily accomplished after the streams are contacted. Fourth, because standard tubular heat exchangers can usually be specified to accomplish the required heat transfer, engineers are hesitant to risk using a relatively new technology such as direct-contact heat exchange. Finally, little information is available that would enable the engineer to design a heat exchange system based on a direct-contact heat exchanger.

This paper addresses the last two concerns by providing insight into how these heat exchangers can be sized and their performance specified. Specifically, this paper presents experimental evidence that supports validation of models for heat exchange and pressure drop in a direct-contact heat exchanger. First, we discuss the data and models available in the literature for heat transfer and then for pressure drop in irrigated packed beds. Particular emphasis is placed on the models used in this paper for comparison purposes. Next, we describe the experimental apparatus used to take the heat transfer and pressure drop data. Experimental procedures and uncertainties are then discussed. Finally, results with discussion and conclusions are presented.

PREVIOUS WORK

All available studies on modeling irrigated packed-bed heat transfer in the literature rely on mass transfer correlations and the analogy between heat and mass transfer. Standish (1968) presented data on heat transfer between hot gases and mercury or cerrobend in a packed bed. Fair (1972) and Bravo and Fair (1982) describe the usage of the heat-mass transfer analogy to predict heat transfer rates in a packed bed given mass transfer coefficients. Mackey and Warner (1972) used the analogy to predict heat transfer rates in a packed bed with downflowing liquid metals and upflowing gases.

Huang (1982) measured heat transfer rates in a packed bed with a mineral spirits/air system and used the analogy to predict the rates. Huang found that the analogy always underpredicted the experimentally determined rates; he attributed this to heat transfer by conduction in the packing (from wet to dry areas), which cannot be accounted for in mass transfer correlations.

Bohn (1985) measured heat transfer rates between air and molten salt in a packed column and used the results to demonstrate the economic benefits of direct-contact heat exchange for that system.

An approach for presenting experimental data followed by several researchers is to measure the heat transfer rate as a function of liquid and gas rate and packing type and size and develop a correlation. The resulting correlation is probably good for the system tested, but applicability to other fluids is questionable. Table 1 presents key elements of several correlations of this type.

Both Huang (1982) and Pohlenz (1947) gave correlations of experimental data relating the volumetric heat transfer coefficient, Ua, to gas rate and liquid rate, G and L, for air-oil systems with 1-in. ceramic Raschig rings:

$$\text{Huang:}\quad Ua = 0.00026\, G^{1.69}\, L^{0.514}$$

$$\text{Pohlenz:}\quad Ua = 0.083\, G^{0.94}\, L^{0.25}$$

(Dimensions for Ua are Btu/h ft^3 ^oF and for G and L, lbm/h ft^2.)

Even for these two very similar systems, we see large discrepancies in determining Ua, e.g., a factor of 4 or more. Possible explanations for the discrepancies include experimental error or a difference in liquid properties. Experimental errors in determining Ua for an irrigated packed column are discussed by Bohn (1983) and can be very large because of close approach

Table 1. Empirical Correlations of Irrigated Packed Bed Heat Transfer

Reference	System	Column Diameter (in.)	Packing
Bennett (1941)	air/oil	8	Raschig rings, 0.5 in.
Hujsak (1947)	air/oil	8	Raschig rings, 0.5 in.
Pohlenz (1947)	air/oil	8	Raschig rings, 1 in.
McAdams (1949)	air/water	4	Raschig rings, 1 in.
Yoshida (1951)	air/water	10	Raschig rings, 1 in., 1.5 in.
Keey (1966)	air/oil	4	Raschig rings, 0.5 in.
Nemunaitis (1975)	air/water	30	Pall rings, 2 in.

temperatures at the top of the column. Liquid properties are not explicit in the above correlations, further demonstrating their limited usefulness for general prediction of heat transfer.

In an attempt to circumvent many of the limitations of the predictive methods previously discussed, Bohn (1987) presented an empirical model for heat transfer in an irrigated packed bed. The application of interest involved high temperatures, thus radiation heat transfer was included. Convection heat transfer was determined from a mass transfer correlation and a correlation that gave the fraction of bed packing wetted by the liquid. Convection from the dry portions of the packing to the gas was also accounted for by incorporation of a fin-effect type of analysis and correlations for heat transfer in packed beds with gas-only flow. It is a main purpose of the present work to test the validity of this empirical model.

Pressure drop and the flooding point in irrigated packed beds are estimated with empirical correlations. White (1935) provides one of the earliest data sets but did not present a correlation of his data because he felt that much more data were needed. He measured pressure drop and determined flooding in a 6-in. column with Raschig rings and an air-water system. Sherwood, Shipley, and Holloway (1938) developed a correlation based on the experimental data available at that time. They showed that the square of the superficial flooding velocity correlated against the ratio of liquid and gas rates. It is a modified version of the Sherwood correlation, provided by Leva (1954) and others, that sees wide usage today. Sarchet (1942) compared the two popular methods of determining the flooding point: visual and pressure drop measurement. He reported that for small packing the two methods give comparable results, but for 1-in. and larger packing the visual flooding velocity may be 20% below the value determined by measuring the pressure drop.

Standish and Drinkwater (1970) modified the Sherwood correlation to include the effect of packing shape via the sphericity, which was defined as a packing shape Inclusion of this empirical shape factor improved agreement between Standish's data and the Sherwood correlation for glass spheres and coke particles in an air-water system. They hypothesized that flooding is caused mainly by pressure gradients in the gas stream that would be influenced by the path the gas must follow through the bed.

Szekely and Mendrykowski (1972) measured flooding critereon for mercury and nitrogen in a 2-in. column packed with glass beads, ceramic cylinders, and saddles. They found that the data fell about an order of magnitude low on the Leva correlation, but agreement with the original Sherwood correlation was quite good. The discrepancy was attributed to the high density and surface tension of the liquid. These results point out that the pressure drop and flooding correlations are based on a relatively small set of gas-liquid systems, and extrapolation of the correlations to new systems can lead to large errors.

Buchanan (1969), Hutton (1974), and Bemer and Kalis (1978) attacked the flooding problem from a different angle. They related the column pressure drop and flooding to the liquid holdup in the bed. In particular, Hutton determined the flooding point as the point where the gradient of liquid rate with holdup is zero. This approach met with partial success by predicting flooding for stacked rings satisfactorily but resulted in large errors for random rings. Buchanan and Bemer and Kalis provide empirical equations that relate the column pressure drop to the holdup and a constant that is characteristic of the packing type and size. Bravo et al. (1986) successfully used the Bemer and Kalis pressure-drop equation to calculate the pressure drop in eight sizes of structured packings from two manufacturers in an air-water system and for a variety of organic liquids in their vapor. Based on the success of the Bemer and Kalis type of pressure drop model, we chose that method for comparison with the experimental pressure-drop data presented in this paper.

DESCRIPTION OF THE EXPERIMENTAL APPARATUS

Tests described in this paper were carried out with the apparatus shown schematically in Figure 1, the molten salt test loop, and in Figure 2, which depicts details of the direct-contact heat exchange column. A mixture of sodium nitrate and potassium nitrate (in a

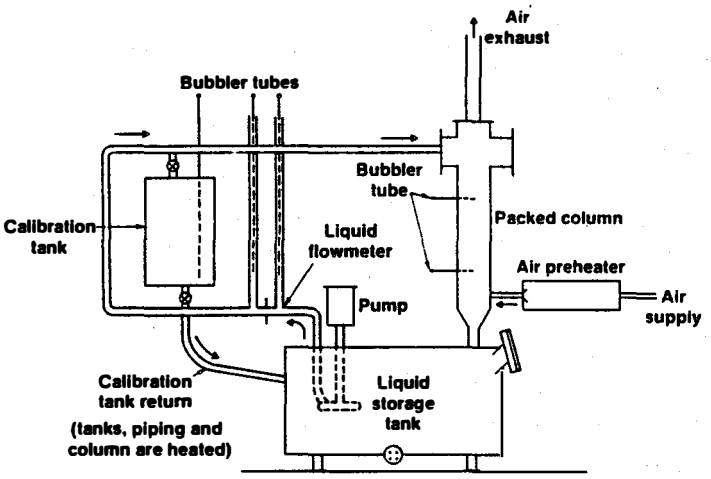

Fig. 1. Direct-contact heat exchange test loop

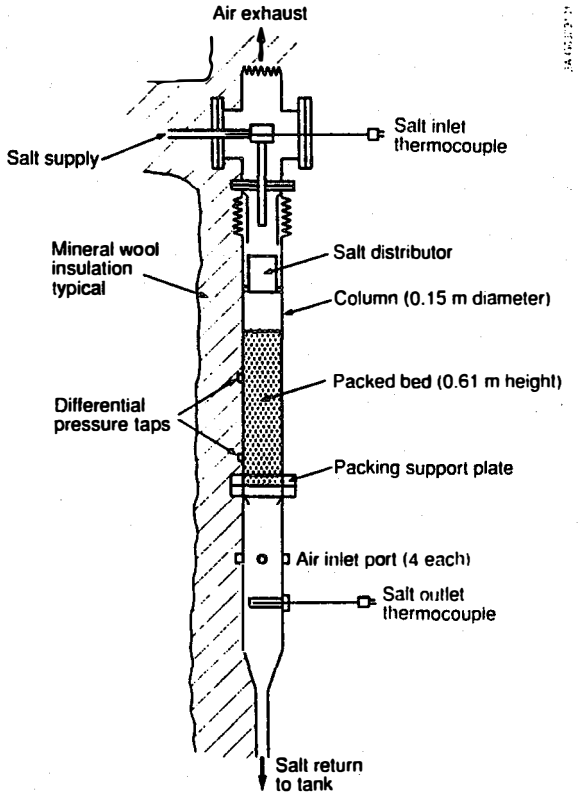

Fig. 2. Vertical cross-section of direct-contact heat exchanger

60/40 wt % ratio, respectively) were used during testing. This salt is presently under consideration as a heat transfer fluid and storage medium for solar thermal central receiver systems that produce electrical power via the steam Rankine cycle. Initial tests were conducted with the eutectic mixture of lithium-sodium-potassium carbonate, which is a candidate storage medium for temperatures in the range from 500° to 900°C. We found that using this salt resulted in exceptionally high column pressure drop from the salt foaming in the column. Presumably, the very high surface tension of the salt, 205 dyne/cm, is responsible for the foaming. Based on a series of flow visualization tests, the nitrate salt, with a surface tension of 105 dyne/cm, did not produce any noticeable foaming over the gas and liquid rates of interest.

An inventory of approximately 1700 kg of molten salt is kept in the storage tank. The salt is pumped out of the tank into the test loop by a cantilever centrifugal pump. Salt flow rate is controlled with a valve welded to the outlet port of the pump housing and actuated from just above the pump mounting flange.

A 1-in. schedule 40 pipe carries the salt to the inlet of the heat exchanger. Immediately downstream of the pump, the salt flows through a wedge flowmeter. Differential pressure across the wedge is sensed as the difference in height of salt in an open vertical pipe on either side of the wedge. A differential bubbler system is used to convert this difference in salt height to a voltage.

Salt flow can be diverted into the calibration tank for calibrating the wedge flowmeter. As salt flows into this calibration tank, the increasing level in the tank is sensed by a bubbler. The rate of change in this bubbler output is compared with the output of the differential bubbler, which senses pressure difference across the wedge. Because the volume of the calibration tank as a function of height is known (by calibration with water), rate of change of salt height in the calibration gives volumetric flow rate directly.

For normal operation in which the salt is directed to the column, refer to Figure 2. The salt enters the column top through a flange on the side of a large T and then enters a small T located inside the large T. The smaller T allows insertion of the calibrated chromel-alumel salt inlet thermocouple into the inlet stream and redirects the salt stream downwards into the salt distributor. The salt distributor is an open-top can with three holes of approximately 1 cm diameter each in the bottom. Clearance between the vertical walls of the distributor and the inside diameter of the column is about 1 cm. We found that this distributor worked satisfactorily flow rates between 60 and 180 cm^3/s. Below 60 the salt issued irregularly from the three holes and tended to attach to the bottom of the distributor. Above 180 cm^3/s the distributor tended to overflow. Within this flow range, three distinct streams issued cleanly from the distributor and spread uniformly over the top of the packed bed. These streams appeared to rapidly spread over the Pall rings within about 30 mm of the top of the bed.

Stainless steel pall rings, 15.9 mm in diameter and height, were used in the column. A total height of 610 mm of randomly dumped rings was used. Important characteristics of these rings are given in Table 2. A corrugated, perforated steel plate supported the rings at the lower column flange in Figure 2. A pair of pressure taps located in the column wall were used with a differential bubbler system to measure column differential pressure during testing. The upper pressure tap was located about one column diameter below the top of the bed to ensure that the liquid and air flows were well distributed. The lower pressure tap was located about one column diameter above the bottom of the packed bed.

Table 2. Characteristics of The Column Packing

Packing type	: Pall rings
Material	: 316 stainless steel
Nominal diameter	: 15.9 mm (5/8 in.)
Specific surface area	: 341 m^2/m^3
Void fraction	: 0.947

Preheated air was introduced into the bottom of the column about 300 mm below the packing support plate. An electric air preheater provided air temperatures up to about 230°C. Four symmetrically arranged inlet ports distributed the air at the base of the column to ensure uniform air flow. Air flow rate was measured with a Datametrics mass flow transducer in the air line just before the air preheater. This transducer was calibrated against an ASME orifice that could be valved into the air line.

Salt outlet temperature was measured with a calibrated chromel-alumel thermocouple inserted into a 25 mm (inside diameter) trough located below the air inlet ports. This trough was designed to ensure that the thermocouple would be bathed in salt that had just left the bottom of the packed bed.

Finally, the salt flows through the bottom of the column back into the storage tank. All test loop piping was heated with tubular heat trace, wrapped with stainless steel foil, and insulated with approximately 150 mm thickness of ceramic fiber insulation. The salt tank was heated with several flat sheathed heaters attached to the tank bottom. The column was heated mainly with flat sheathed heaters formed in a circular shape and attached to the column outside diameter with clamps.

All data, with the exception of the column differential pressure, were acquired with an Ithaco Compudas data acquisition system. Column differential pressure data were recorded on a strip-chart recorder. For trend indication, the data acquisition system sent, via digital-to-analog convertors, several critical data channels to the strip-chart recorder.

TEST PROCEDURE

On the basis of a great deal of testing, we determined that the best comparison between the predictions of the heat transfer model and experimental data would be that of the heat transferred from the salt. In earlier attempts to measure the volumetric heat transfer coefficient, Bohn (1983) showed that large uncertainties result, primarily because of the difficulty in measuring the air outlet temperature, which typically is very close to the salt inlet temperature. Measurement errors in the airstream are large because of radiation errors and because salt droplets are usually entrained in the airstream. Measuring the salt heat transfer is relatively simple, requiring only a measure of the salt flow rate and terminal salt temperatures. It is necessary, however, to account for heat transfer from the salt that occurs in regions of the column other than in the packed bed.

Included in these additional heat transfer paths are the heat lost from the salt to the column walls and the heat transferred to the air in the region below the packed bed. Since the air exiting the top of the packed bed is very nearly in thermal equilibrium with the salt entering from the salt distributor, we neglect salt-to-air heat transfer above the packed bed. Our experimental procedure allowed us to determine the loss from the salt to the column. The loss in the region

below the packed bed was estimated and is included in our statement of experimental uncertainty. Data were reduced according to the following equation:

$$Q_{sm} = \dot{m}_s C_s (T_{si} - T_{so}) - Q_{loss} \quad . \qquad (1)$$

The term on the left side of equation (1) is the heat transfer from the salt to the air, which occurs in the packed bed. The first term on the right side of the equation is the salt heat loss determined from the measured salt flow rate and temperature drop. The second term on the right side of the equation represents the two sources of heat loss from the salt stream just discussed and may be expressed as follows:

$$Q_{loss} = \dot{m}_s C_s (T_{si} - T_{so})\big|_{C=0} + Q_{outlet} \qquad (2)$$

Thus, the loss from the salt to the air in regions of the column other than the packed bed include losses to the column wall, which is measured after every data point as described later, and heat loss below the packed bed, Q_{outlet}, which is estimated. It is the term on the left side of equation (1) that we would like to deduce from the experimental data and compare with the heat transfer model.

To ensure that salt could be successfully pumped through the test loop, the loop was brought up to 400°C over a period of about two days and left at that temperature for an additional day. During this period, a low flow of air was bled through the air preheater (which was turned on at a low power setting) and column to heat up the preheater and air piping. We then shut off the air flow and started the salt flow. After several hours, the salt and the column reached equilibrium as evidenced by the steadiness of the salt inlet and outlet temperatures.

After this equilibrium was established, air flow was started again. Typically, a new equilibrium would be established within 10 minutes, again as evidenced by steady salt inlet and outlet temperatures. At this point, the data acquisition system would be instructed to record 30 samples from each channel, to average each channel, and to calculate the standard deviation for each channel. Based on these average values, the gross heat loss from the salt could be calculated according to the first term on the right side of equation (1).

After these data were recorded, the air flow was turned off. A new equilibrium would be reached within three minutes, which corresponded to the heat loss from the salt through the column walls in the absence of air flow, e.g., the first term on the right side of equation (2). The indicated column pressure differential under these conditions equals the bubbler offset signal since no air is flowing through the column to create a differential pressure. Again, 30 readings would be taken, and based on the average salt flow rate and salt inlet and outlet temperatures, the heat loss from the salt would be calculated and subtracted from the gross heat loss per equation (1). The column differential pressure recorded with air flow is reduced by the value recorded with no air flow to give the net column differential pressure.

After establishing a higher air flow rate, the procedure would be repeated. The sequence of operating conditions usually included starting at low air flow and increasing the air flow in steps until the column differential pressure exceeded approximately 1000 Pa/m or until unsteady operation indicated the onset of flooding. Then, the air flow would be reduced in steps with the same salt flow. After this sequence was completed a new salt flow would be set and the procedure repeated. At each data point, operating conditions including air flow rate, salt flow rate, air inlet temperature, and salt inlet temperature, were entered into the heat transfer model. The pressure drop model and predicted values of the salt heat transfer and column pressure drop were then determined for comparison with the data.

The first series of tests were intended to map out the column differential pressure. These tests were performed with an air inlet temperature in the range from 196° to 250°C and a salt inlet temperature in the range from 306° to 360°C. Heat transfer was not measured during these tests.

The main test series involved simultaneous measurement of heat transfer and column differential pressure at a single salt inlet temperature of approximately 400°C, salt flows ranging from 60 to 165 cm^3/s, and air flows ranging from 280 to 1100 slpm. Given the column inside diameter, these flow rates correspond to a liquid rate of approximately 6 to 18 kg/m^2 s and a gas rate of 0.3 to 1.2 kg/m^2 s. Resulting net salt heat transfer ranged from 1000 to 4500 watts. Resulting column differential pressure ranged from 163 to 1225 Pa/m. Generally, packed columns are operated at approximately 400 Pa/m with 1200 Pa/m considered to be the point where flooding commences. Thus, our range of operating conditions fully covered the operating map for a packed column.

UNCERTAINTY ANALYSIS

Referring to equation (1), the reported salt heat transfer rate was determined from the total heat lost by the salt less column heat losses and the internal loss from the salt to the air below the packed bed. Since the column heat losses were determined after each data point, this bias error was measured and accounted for in the equation. The internal loss was estimated as follows. Based on our observations of the flow below the packing support plate, we model the salt flow in this region of the column as consisting of five rivulets of 5 mm diameter. Given the salt flow rate, the salt velocity in these rivulets can be determined. Given the air flow rate and inlet temperature, air velocity can be determined. Using the relative velocities between the air and the salt and treating the heat transfer between the two streams as that of flow over a flat plate, a heat transfer coefficient can be determined. To be conservative, we doubled this heat transfer coefficient to account for rippling or other motion in the rivulets, which may enhance this heat loss mechanism. From the measured salt outlet temperature and measured air inlet temperature, an estimate of the heat loss is determined to be approximately 3% of the gross salt heat loss. We include this loss as a negative bias error in determining the overall uncertainty in the heat transfer measurement.

Other uncertainties in equation (1) that must be considered include errors in the salt flow rate measurement, the specific heat of the salt, and the salt inlet-to-outlet temperature difference. By far, the largest contributor to the overall uncertainty is the problem in determining salt inlet-to-outlet temperature difference. As discussed previously, the salt inlet temperature and outlet temperature were measured with calibrated chromel-alumel thermocouples. In estimating the uncertainty in measuring this temperature difference, the sources of error considered included (i) uniformity of the fluid bed used to calibrate the thermocouples, ±0.02°C; (ii) standard error of estimating the curve-fit to the thermocouple calibration data, ±0.34°C; (iii) temperature differences from one channel to another at the thermocouple terminal strip, <±0.005°C; (iv) errors due to the thermocouple extension wire, ±0.05°C; and (v) resolution of the analog-to-digital conversion system, ±0.38°C.

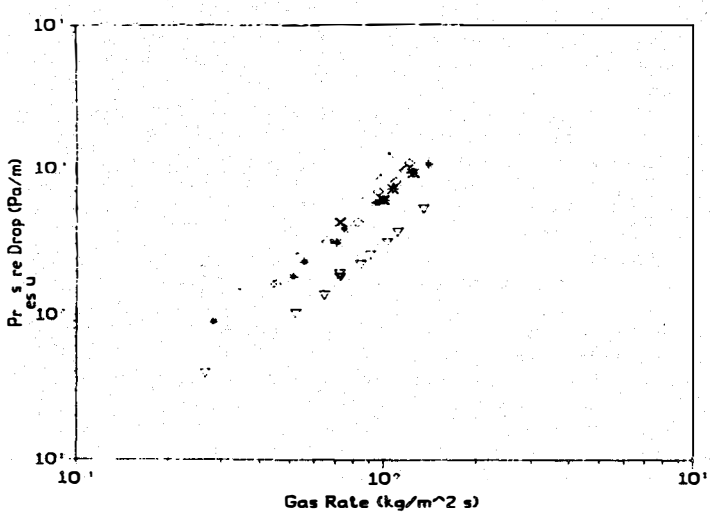

Fig. 3. Pressure drop versus gas rate, $196 < T_{ai} < 250°C$, $306 < T_{si} < 360°C$, ▽ is L 0, * is $5.7 < L < 7.2$, ◇ is L 12.4, × is L = 18.2.

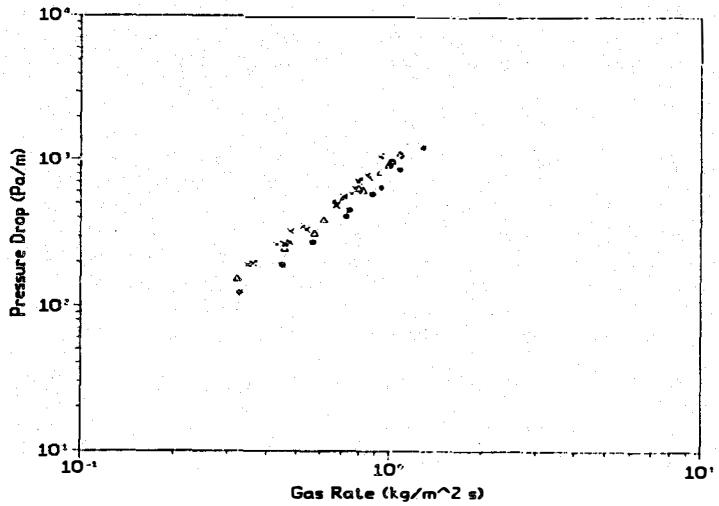

Fig. 4. Pressure drop vs. gas rate during heat transfer tests, $T_{ai} \approx 220°C$, $T_{si} \approx 420°C$, * is L = 6.5, ◇ is L = 12.5, Δ is L = 14.5, × is L = 17.5.

A precision error of ±0.32°C was also estimated based on temperature data recorded during an actual run. Thermocouple immersion errors were neglected because care was taken with how the thermocouples were installed in the column to simulate, as closely as possible, the immersion used during thermocouple calibration. Bias errors during calibration, which cancel out when calculating the difference in temperature between the salt inlet and outlet thermocouples, were ignored. These include the uncertainty in the quartz thermometer and ice point reference used in calibrating the thermocouples.

Other errors in applying equation (1) include the salt flow rate measurement, ±2.4% bias error and ±0.6% precision error, and the uncertainty in the salt specific heat, ±3% bias error. Since the overall heat transfer is reported as a function of air flow rate, we determined that the air flow measurement is associated with a ±3.7% bias error and a ±0.2% precision error. Total estimated uncertainty on the reported salt heat transfer rate is ±29%.

Column differential pressure was measured with a bubbler system as discussed earlier. This bubbler was calibrated against a micromanometer, which has a range of ±5000 Pa and a resolution of 0.25 Pa. As described in the Test Procedures section, the column differential pressure was measured before the air flow was started to get the bubbler bias for zero air flow. This source of bias error was therefore eliminated. Based on the curve-fit of the calibration data and the precision errors during an actual run, we estimate that the overall uncertainty in the column differential pressure measurement is ±9%.

RESULTS

Pressure Drop

A first series of tests was run to determine the pressure drop behavior of the column over a range of gas and liquid rates. Figure 3 presents the results in which column pressure drop is plotted against gas rate. For these tests the air inlet temperature varied from 196°C to 250°C and the salt inlet temperature varied from 306°C to 360°C. The behavior depicted by the figure is quite typical of irrigated packed beds. For L = 0, the pressure drop increases approximately with $G^{1.67}$. At a given gas rate, a large increase in pressure drop results from an increase in L from 0 to about 6 kg/m^2 s, and further increases in L produce relatively small increases in pressure drop. As L increases, the exponent on G does not seem to vary significantly. For the highest liquid rate, the effect of column flooding can be clearly seen; as G is increased beyond about 0.8 kg/m^2 s, the pressure drop begins to increase more rapidly than the linear behavior seen on the log-log plot. This behavior is also visible, to a lesser extent, for the L = 12 kg/m^2 s data, but not for the L = 6 data.

Results of Figure 3 were used to guide the heat transfer tests by showing that a pressure drop of greater than approximately 1000 Pa/m indicated column flooding. Pressure drop was also measured during the heat transfer tests, and those data are plotted in Figure 4. The main difference between these data and the data in Figure 3 is that the air temperature was higher in the former, thus producing a slightly higher column pressure drop. Also, the maximum pressure drop for L = 17.5 kg/m^2 s was lower during the heat transfer tests to avoid flooding, and for the two lower liquid rates, slightly higher pressure drop maximums were tested during the heat transfer tests. Thus, the effects of flooding can be seen on the heat transfer data, which is discussed in the following section.

As discussed in the section on modeling, we compared the pressure drop with the model of Bemer and Kalis (1978). Results of this comparison are presented in Figure 5. This graph includes not only the first series of tests in which only the pressure drop behavior of the column was determined but also the heat transfer tests in which column pressure drop was determined simultaneously with heat transfer. In total, 110 data points are included. The measured pressure drop is compared with the predicted pressure drop in the figure. Predicted pressure drop was determined from the Bemer and Kalis model using the indicated liquid and gas flow rates and by using properties of the two fluid streams determined at the average of their inlet and outlet temperatures. In the case of L = 0, air properties were determined at the air inlet temperature.

Critical properties of the packing used during the tests, which are needed for the Bemer and Kalis model, include the specific surface area and the void fraction; Table 2 gives numerical values for these and other properties of the packing. The figure shows good

agreement between the data and the model. Standard deviation between the experimental data and the model is 18% for all data points. Bemer and Kalis found that literature data fell within ±20% of their model for metal Pall rings ranging in size from 15 mm to 50 mm. Note that the agreement is good even for a pressure drop as high as 1250 Pa/m, the highest for which we took data and for which column flooding was indicated.

Although the available column flooding correlations were not compared with experimental data, our operational experience indicates that a pressure drop of 1200 Pa/m is a definite upper limit and 1000 Pa/m is probably a safe upper limit for column operation.

Heat Transfer

Figure 6 presents a comparison of the measured salt heat transfer with the calculated salt heat transfer in the form of a parity plot. As discussed previously, the operating conditions for each experimental point were entered into the heat transfer model to predict the expected salt heat transfer for those operating conditions. The results in Figure 6 demonstrate that the comparison is quite good. Overall, for the 54 data points plotted, the standard deviation between the predicted and measured values is 22%. Given that the mass transfer correlation upon which the model is based has a ±37% uncertainty, this deviation between model and experimental data appears reasonable.

At the lower salt flow rates a larger salt temperature difference results for a given heat transfer, and the experimental uncertainties are smaller. This is consistent with suggesting that the model compares favorably with the data because the data for the lowest liquid rate, which should have the lowest experimental uncertainty, compare very closely with the parity line in Figure 6. As pointed out in the discussion of the heat transfer model, a change in salt flow rate mainly influences the fraction of packing, which is wetted, and this effect is fairly small over the range of data presented, typically from 0.65 at L = 6 kg/m^2 s to 0.85 at L = 18 kg/m^2 s. Thus, it does not appear that liquid rate should affect heat transfer as strongly as indicated by the data.

For the two lower salt flows tested, the predicted heat transfer is significantly larger than the measured heat transfer at high heat transfer rates. This is because the high heat transfer rates result from high gas rates, which, in turn, produce high column pressure drop and ultimately column flooding. Column flooding leads to poor liquid distribution and liquid backmixing and yields lower heat transfer. The heat transfer model does not account for these additional complexities and, therefore, overpredicts the salt heat transfer for high gas rates.

Figure 7 demonstrates the dependence of salt heat transfer on gas rate. Taken in aggregate, the data follow approximately

$$Q_s \sim G^{0.92}$$

The figure also demonstrates the lack of dependence of salt heat transfer on liquid rate. Within the experimental scatter, no discernable dependence exists. For the two lower liquid rates, 6.6 and 12.3 kg/m^2 s, the effects of column flooding can be clearly seen as the heat transfer ceases to increase after a gas rate of approximately 1.0 kg/m^2 s. Recall from Figure 4 that the maximum column pressure drop for these two liquid rates was about 1000 Pa/m. At the highest liquid rate, 17 kg/m^2 s, this flooding effect is not observed because, as explained earlier, the column pressure drop

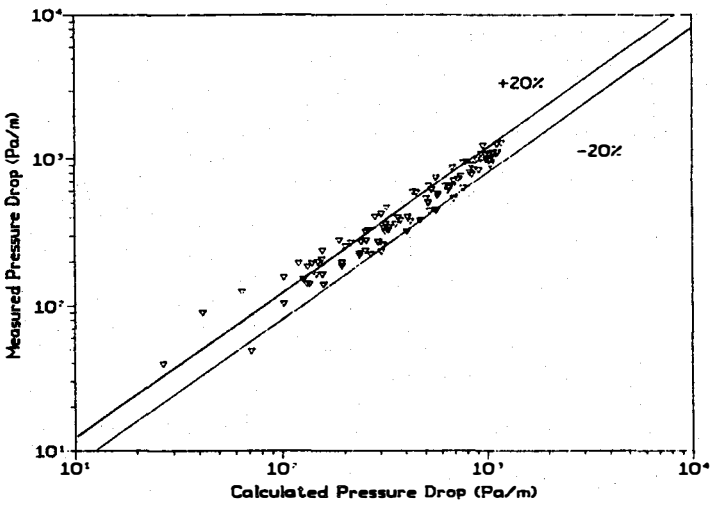

Fig. 5. Comparison of measured and predicted pressure drop

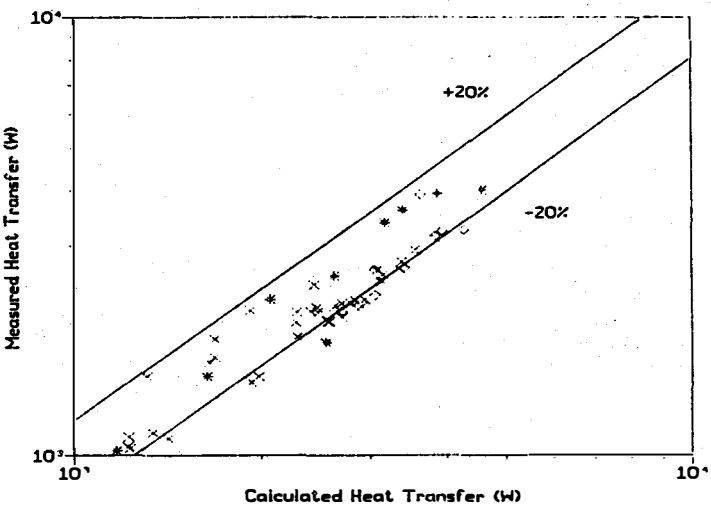

Fig. 6. Comparison of measured and predicted heat transfer, $T_{ai} \approx 220°C$, $T_{si} \approx 420°C$, * is L = 6.6, ◇ is L = 12.3, × is L = 17.

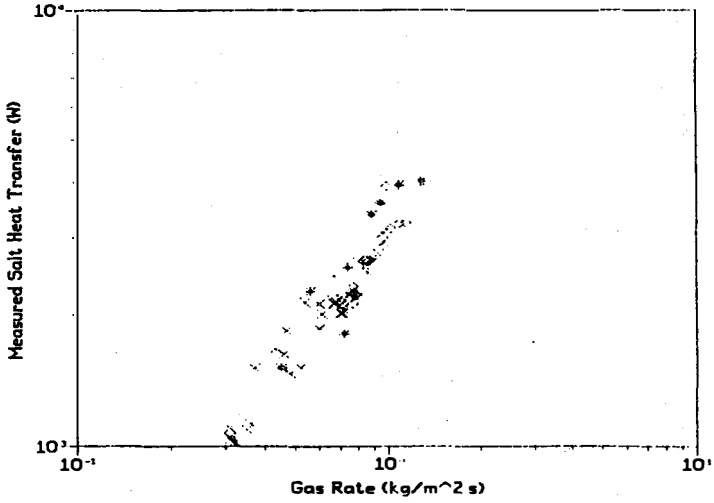

Fig. 7. Heat transfer versus gas rate, * is L = 6.6, ◇ is L = 12.3, × is L = 17.

was limited to just below flooding during the heat transfer tests for this high liquid rate.

We observed that in the gas rate range from 0.35 to 0.55 kg/m^2 s, the data repeatability was poor. As an example, note the data for L = 17 kg/m^2 s and G = 0.36 where the three data points are Q_s = 1092, 1126, and 1513 W. The higher point is nearly 50% above the other two. The pressure drop for these three points was 193, 198, and 204 Pa/m, which are quite comparable. In this gas rate range, the column appeared to operate at least as steady as for other gas rates. Similar erratic behavior can be seen for L = 17 kg/m^2 s and G = 0.53 kg/m^2 s where the Q_s differs by about 40% between the two data points. Thus, it appears that in the gas rate range of 0.35 to 0.55 kg/m^2 s, the column operated in one of two modes with significantly different heat transfer. Based on the data for L = 17 kg/m^2 s and G > 0.6 kg/m^2 s, i.e., beyond this two-mode regime, the column seems to follow the data for the lower heat transfer mode.

DISCUSSION, CONCLUSIONS, AND FUTURE RESEARCH

Direct-contact heat transfer between a preheated stream of air and a stream of molten nitrate salt in a packed bed was measured and compared with an empirical model. The range of gas rates and resulting pressure drop fully covered the operating range for irrigated packed beds. The model and experimental data agree to within the uncertainty in the empirical correlations used to produce the model and the experimental uncertainties. Agreement between a model for the pressure drop in the packed bed and the experimental data was also good.

These two models then provide a relatively simple way to determine the performance of an irrigated packed bed, direct-contact heat exchanger. An overall volumetric heat transfer coefficient, Ua, can be determined from the heat transfer model given gas and liquid properties, temperatures, flow rates, and the details of the packing. If the heat exchanger terminal temperatures are known, Ua can be used directly to determine the heat duty or heat exchanger size from

$$Q_s = UaV_{hx}\Delta T_{LM} \quad . \tag{3}$$

where

$$\Delta T_{LM} = \frac{(T_{si} - T_{ao}) - (T_{so} - T_{ai})}{\ln \frac{(T_{si} - T_{ao})}{(T_{so} - T_{ai})}}$$

If the fluid outlet temperatures are not known, they can be determined from charts of heat exchanger effectiveness for a counterflow heat exchanger. In place of the number of transfer units, which appears on the abscissa of the chart, we would use

$$Ntu = H/Htu \quad , \tag{4}$$

where Htu is commonly called the height of a transfer unit:

$$Htu = Max\ (HUa/GC_p,\ HUa/LC_s) \quad . \tag{5}$$

Using the Bemer and Kalis model for pressure drop, the heat exchanger design can be completed. That is, the engineer can perform trade-off studies of heat exchanger size and cost versus operating costs, which will be related primarily to the pressure drop.

Since one of the major conclusions of the heat transfer model was that radiation exchange does not play an important role in an irrigated packed bed heat exchanger, a wide range of operating temperatures needs to be tested to validate the model in which radiation is neglected. Since a commercial heat exchanger would most likely operate with significantly lower liquid rates than those presented in this work, a range of liquid rates needs to be tested to fully validate the model. Different packings should also be tested to make sure that the geometric treatment of the packing conduction heat transfer is valid. Finally, testing at a larger scale is required before the model can be fully validated and before acceptance of the concept by practicing engineers can be expected.

ACKNOWLEDGMENT

The work described in this paper is supported by the U.S Department of Energy, Energy Storage and Distribution Division.

REFERENCES

Bohn, M. S., 1983, "Air/Molten Salt Direct-Contact Heat-Transfer Experiments and Economic Analysis," SERI/TR-252-2015, Solar Energy Research Institute, Golden, CO.

Bohn, M. S., 1985, "Air/Molten Salt Direct Contact Heat Transfer," Journal of Solar Energy Engineering, Vol. 107, pp. 208-214.

Bohn, M. S., 1987, "Analytical Model of an Irrigated Packed-Bed Direct Contact Heat Exchanger at High Temperature," Proceedings of the 2nd ASME-JSME Thermal Engineering Conference, ASME, Honolulu, HI.

Bemer, G. G., Kalis, G. A. J., 1978, "A New Method to Predict Hold-up and Pressure Drop in Packed Columns," Trans. Instn. Chem. Engrs., Vol. 56, pp. 200-204.

Bennett, G. A., 1941, MS thesis, Case Institute.

Buchanan, J. E., 1969, "Pressure Gradient and Liquid Holdup in Irrigated Packed Towers," I&EC Fundamentals, Vol. 8, pp. 502-511.

Bravo, J. L., Fair, J. R., 1982, "Generalized Correlations for Mass Transfer in Packed Distillation Columns," Ind. Eng. Chem. Process Des. Dev., Vol. 21, pp. 162-170.

Bravo, J. L., Rocha, J. A., and Fair, J. R., 1986, "Pressure Drop in Structured Packings," Hydrocarbon Processing, March, pp. 45-49.

Fair, J. R., 1972, "Designing Direct Contact Coolers/Condensers," Chemical Engineering, June, pp. 91-100.

Huang, C., 1982, "Heat Transfer by Direct Gas-Liquid Contacting," M.S. Thesis, University of Texas, Austin, TX. To appear in Heat Transfer Engineering, 1988.

Hujsak, K. L., 1947, "The Transfer of Heat Between Air and a Nonvolatile Oil in a Packed Tower," M.S. Thesis, Massachusetts Institute of Technology, Cambridge, MA.

Hutton, B. E. T., Leung, L. S., Brooks, P. C., 1974, "On Flooding in Packed Columns," Chemical Engineering Science, Vol. 29, pp. 493-500.

Keey, R. B., 1966, "Fluid-Fluid Heat Transfer in a Packed Column," Proceedings, Third International Heat Transfer Conference, Vol. 4, pp. 322-328.

Leva, M., 1954, "Flow Through Irrigated Dumped Packings," Chem. Engng. Progr. Symp. Ser., Vol. 50, pp. 51-59.

McAdams, W. H., Pohlenz, J. B., St. John, R. C., 1949, "Transfer of Heat and Mass Between Air and Water in a Packed Tower," Chem. Eng. Prog., Vol. 45, pp. 241-252.

Mackey, P. J., Warner, N. A., 1972, "Heat Transfer Between Dispersed Liquid Metals and Gases in Packed

Beds," Metallurgical Transactions, Vol 3, pp. 1807-1816.

Nemunaitis, R. R., Eckert, J. S., 1975, "Heat Transfer in Packed Towers," Chem. Eng. Progr., Vol. 71, pp. 60-67.

Pohlenz, J. B., 1947, "Heat and Mass Transfer in Packed Towers," Ph.D. Thesis, Massachusetts Institute of Technology, Cambridge, MA.

Sarchet, B. R., 1942, "Flooding Velocities in Packed Towers," Transactions of American Institute of Chemical Eng., Vol. 38, pp. 283-304.

Sherwood, T. K., Shipley, G. H., Holloway, F. A., 1938, "Flooding Velocities in Packed Columns," Ind. Eng. Chem., Vol. 30, pp. 765-769.

Standish, N., 1968, "Heat Transfer in Liquid Metal Irrigated Packed Beds Countercurrent to Gases," Transactions of the Metallurgical Society of AIME, Vol. 242, pp 1733-1740.

Standish, N. and Drinkwater, J., 1970, "The Effect of Particle Shape on Flooding Rates in Packed Columns," Chemical Engineering Science, Vol. 25, pp. 1619-1621.

Szekely, J. and Mendrykowski, J., 1972, "On the Flooding Criteria for Liquids with High Density and High Interfacial Tension," Chemical Engineering Science, Vol. 27, pp. 959-963.

White, A., 1935, "Pressure Drop and Loading Velocities in Packed Towers," Transactions of American Institute of Chemical Eng., Vol. 31, pp. 390-408.

Yoshida, F., Tanaka, T., 1951, "Air-Water Contact Operations in a Packed Column," Ind. Eng. Chem., Vol. 43, pp. 1467-1473.